Synthesis and characterisation of some hexanuclear heterometallic clusters containing arene ligands; the crystal and molecular structures of $RuOs_5(CO)_{15}(\eta^6\text{-}C_6H_6)$ and $RhOs_5(CO)_{15}(\eta^5\text{-}C_5Me_5)$

Richard K. Henderson, Patricia A. Jackson, Brian F. G. Johnson, Jack Lewis* and Paul R. Raithby

University Chemical Laboratory, Lensfield Road, Cambridge CB2 1EW (UK)

Abstract

Treatment of the pentaosmium dianionic cluster $[Os_5(CO)_{15}]^{2-}$ (**1**) with either one equivalent of the dication $[Ru(\eta^6\text{-}C_6H_6)(MeCN)_3]^{2+}$ (**2**), or one equivalent of $[Rh(\eta^5\text{-}C_5H_5)(MeCN)_3]^{2+}$ (**3**), in dichloromethane, at 0 °C, affords two isomeric forms of the cluster $RuOs_5(CO)_{15}(\eta^6\text{-}C_6H_6)$ (**4**), or three isomeric forms of $RhOs_5(CO)_{15}(\eta^5\text{-}C_5Me_5)$ (**5**), respectively. One isomeric form of each cluster (**4a** and **5a**) has been characterised crystallographically. The structures of **4a** and **5a** both contain a bicapped tetrahedral metal core in which the heteroatom occupies one of the two capping positions; this is in accord with the geometry predicted for a six metal atom cluster with 84 valence electrons. Reduction of the cluster **4** with K/Ph_2CO, in tetrahydrofuran, affords the octahedral dianionic cluster $[RuOs_5(CO)_{14}(\eta^6\text{-}C_6H_6)]^{2-}$ (**6**). When this dianion is treated with $HBF_4 \cdot Et_2O$ decomposition occurs, and small amounts of the parent cluster **4** are regenerated. Treatment of **6** with $[AuPEt_3]Cl/Tl[BF_4]$ gives the neutral cluster $RuOs_5(CO)_{14}(\eta^6\text{-}C_6H_6)(AuPEt_3)_2$ (**7**).

Introduction

The ionic coupling reactions of binary carbonyl clusters, leading to the formation of higher nuclearity homo- and heteronuclear clusters of the platinum group metals have met with limited success. Redox condensation routes, addition of metallates to metal halides and addition to coordinatively unsaturated clusters are more fruitful reactions of ionic substrates [1]. In particular, there are relatively few reports of the use of higher clusters of the iron triad in ionic coupling reactions with transition metal cations, although there are many examples of the addition of Au, Cu and Ag cationic species [2]. In order to improve the efficacy and generality of this route to heterometallic clusters of high nuclearity, we have sought to exploit the rationale of the isolobal analogy and have investigated the reaction of cationic precursors with polyhedral anionic cluster fragments. For example, the cation $[Ru(\eta^6\text{-}C_6H_6)(MeCN)_3]^{2+}$, which is a source of '$Ru(C_6H_6)$', is isoelectronic to a twelve electron capping unit. We describe here the results of the coupling of the trigonal bipyramidal dianion $[Os_5(CO)_{15}]^{2-}$ with $[RM(MeCN)_3]^{2+}$ ions, where RM = '$Ru(\eta^6\text{-}C_6H_6)$' and '$Rh(\eta^5\text{-}C_5Me_5)$', to generate heterometallic analogues of the well-known binary carbonyl cluster $Os_6(CO)_{18}$ [3]. The use of arene containing active fragments is also of interest because of our current interest in the bonding modes adopted by benzene and related arenes when coordinated to polynuclear metal carbonyl complexes [4].

*Author to whom correspondence should be addressed.

Experimental

Although many of the reaction products are air stable, all manipulations were performed under an atmosphere of dry, oxygen-free, dinitrogen, using standard Schlenk and vacuum-line techniques. Solvents were distilled prior to use, under an inert N_2 atmosphere, over the appropriate drying agents.

Routine separation of products was performed by thin layer chromatography, using commercially prepared glass plates, precoated to 0.25 mm thickness with Merck Kieselgel 60 F_{254}, as supplied by Merck; or, using laboratory prepared glass plates to 1 mm thickness with Merck Kieselgel 60 PF_{254}.

IR spectra were recorded as solution spectra, on a Perkin-Elmer 983 grating spectrophotometer, or a Perkin-Elmer 1710 Fourier transform spectrophotometer,

0020-1693/92/$5.00

using 0.5 mm NaCl or CaF_2 cells. NMR spectra were recorded on Bruker WM250 MHz or Bruker AM400 FT spectrometers, using an internal ^2H lock. Mass spectra were recorded on AEI MS12, AEI MS902 or Kratos AEI MS890 spectrometers. Elemental analyses were performed by the microanalytical service within the department.

The ions $[Ru(C_6H_6)(MeCN)_3]^{2+}$, $[Rh(C_5Me_5)(MeCN)_3]^{2+}$, $[Os_5(CO)_{15}]^{2-}$ and $[AuPEt_3]^+$ were prepared by literature procedures [5–8].

Preparation of $RuOs_5(CO)_{15}(C_6H_6)$ (4a, 4b)

$[Ru(C_6H_6)(MeCN)_3](PF_6)_2$ (18 mg, 0.036 mmol) was dissolved in acetone (2 ml), and the solution degassed and cooled to −78 °C in a dry-ice/acetone bath. A solution of $[(Ph_3P)_2N]_2[Os_5(CO)_{15}]$ (60 mg, 0.024 mmol) in CH_2Cl_2 (10 ml) was added dropwise over a period of 10 min. The solution was allowed to warm to room temperature and stirred for a further 0.5 h. The solvent was removed *in vacuo*, and the CH_2Cl_2 soluble residue purified by TLC, using CH_2Cl_2:hexane (50:50) as eluant. The major dark band (R_f0.6) was extracted and crystallised from CH_2Cl_2:hexane (50:50) to yield a red–brown crystalline product (**4a**) (*c.* 60% yield). The second isomer **4b** was separated similarly (*c.* 10% yield).

Preparation of $RhOs_5(CO)_{15}$ (C_5Me_5) (5a, 5b, 5c)

The methodology is analogous to that applied for **1**, using $[Rh(C_5Me_5)(MeCN)_3](SbF_6)_2$ (10 mg, 0.012 mmol, 1.5 equiv.) in MeCN (5 ml) and $[(Ph_3P)_2N]_2[Os_5(CO)_{15}]$ (20 mg, 0.008 mmol) in dichloromethane (5 ml). Three bands (R_f 0.6, brown (**5a**); R_f 0.55, brown (**5b**); R_f 0.5, brown (**5c**)) were extracted and crystallised from dichloromethane/hexane (50:50) to yield the red–brown crystalline compounds **5a** (*c.* 20% yield), **5b** (*c.* 10% yield) and **5c** (*c.* 10% yield). The band at R_f 0.55 initially appeared as a blue crystalline product which rapidly turned brown on elution.

Reduction of $RuOs_5(CO)_{15}(C_6H_6)$ to the dianion 6

Method 1. To a cooled solution of **1** (20 mg) in freshly distilled tetrahydrofuran (3 ml, −78 °C) was added dropwise a solution of potassium (180 mg) and benzophenone (840 ml, 1 equiv.) in the same solvent (2 ml). After stirring for 1 h the solvent was removed under vacuum to leave the product '$K_2[RuOs_5(C_6H_6)(CO)_{15}]$' as a brown oil. This oil was dissolved in dichloromethane and used without further purification in all the other experiments.

Method 2. Complex **1** (25 mg) was dissolved in tetrahydrofuran (3 ml) and shaken with freshly prepared Na/Hg. After separation of the amalgam and removal of solvent under vacuum the oily residue was dissolved in dichloromethane and used without further purification.

Preparation of $RuOs_5(CO)_{15}(C_6H_6)(AuPEt_3)_2$ (7)

The dianion, $[RuOs_5(C_6H_6)(CO)_{15}]^{2-}$ (**5**) (as its potassium salt) (20 mg, 0.17 mmol), was prepared as above and redissolved in dichloromethane (5 ml). The solution was added dropwise to a suspension of $[AuPEt_3]Cl$ (13 mg, 0.037 mmol, 2.2 equiv.) and $TlPF_6$ (13 mg, 0.034 mmol, 2 equiv.) in dichloromethane (5 ml), at −78 °C. The solution was observed to change to a deep brown colour. It was allowed to warm to room temperature and stirred for a further 0.5 h. The solvent was removed *in vacuo*, and the dichloromethane soluble residue purified by TLC, using dichloromethane:hexane (50:50) as eluant. The bright red band (R_f 0.5) was extracted and crystallised from dichloromethane:hexane as deep red needles, $RuOs_5(CO)_{15}(C_6H_6)(AuPEt_3)_2$ (**7**) (*c.* 80% yield).

Reaction of $[RuOs_5(C_6H_6)(CO)_{15}]^{2-}$ (6) with $HBF_4 \cdot Et_2O$

To a solution of the dianion $[RuOs_5(C_6H_6)(CO)_{15}]^{2-}$ (**6**) (25 mg) in dichloromethane (5 ml) was added a solution of $HBF_4 \cdot Et_2O$ in the same solvent and the solution stirred under CO (1 atm.) for *c.* 0.5 h. After removal of the solvent the solid residue was chromatographed by TLC using a dichloromethane:hexane mixture to separate small amounts of compounds **4a** and **4b**.

X-ray crystal structure determination of $RuOs_5(\eta^6\text{-}C_6H_6)(CO)_{15}$ (4a)

Crystals of **4a** were grown by slow evaporation of a dichloromethane:hexane (60:40) mixture and a suitable single crystal was mounted on a glass fibre with epoxy resin.

Crystal data

$C_{21}H_6O_{15}Os_5Ru$, $M = 1550.33$, monoclinic, space group $P2_1/n$ (alt. setting $P2_1/c$, No. 14), $a = 9.517(5)$, $b = 18.329(10)$, $c = 15.464(14)$ Å, $\beta = 92.91(6)°$, $V = 2694(6)$ Å^3 (by least-squares refinemcnt of diffractometer angles from 25 automatically centred reflections in the range $15 < 2\theta < 25°$, $\lambda = 0.71073$ Å), $Z = 4$, $D_c = 3.82$ g cm^{-3}, D_m = not measured, $F(000) = 2704$. Purple platelet. Crystal dimensions: $0.05 \times 0.16 \times 0.36$ mm, μ(Mo Kα) = 240.98 cm^{-1}, $\mu R = 2.29$.

Data collection and processing

Nicolet R3mV diffractometer, 96-step ω–2θ scan mode, with scan range from 0.9° below Kα_1 to 0.9° above Kα_2, with ω scan speeds in the range 2.0–19.53°/min, graphite-monochromated Mo Kα radiation, 3329 reflections measured ($5.0 < 2\theta < 42.0°$, $+h$, $+k$, $\pm l$), 2857 unique (merging $R = 0.019$ after a semi-empirical absorption correction based on an ellipsoid model and 383 scan data (maximum minimum transmission factors

0.019, 0.002), giving 1330 with $F > 6\sigma(F)$. Three check reflections showed significant variations in intensity during data collection, which were caused by repeated instrument malfunction, and which could not be corrected during data reduction.

Structure solution and refinement

Centrosymmetric direct methods (Os and Ru atoms) followed by Fourier difference techniques for the remaining non-hydrogen atoms. Full-matrix least-squares refinement with Os and Ru atoms anisotropic. The weighting scheme $w = [\sigma^2(F) + 0.008F^2]^{-1}$, with $\sigma(F)$ from counting statistics, gave satisfactory agreement analyses. Additional positional constraints using, DFIX, were placed on the carbonyl ligands, with Os–C 1.90(1) and 1.16(1) Å. Final R and R_w values were 0.091 and 0.097, and the goodness of fit parameter $S = 1.33$. Highest peak in the final difference map 3.5 e Å^{-3} close to the metal atom positions. Final fractional atomic coordinates are presented in Table 1. Computations were carried out on a MicroVax II computer using the SHELXTL PLUS package [9].

X-ray crystal structure determination of $RhOs_5(\eta^5\text{-}C_5Me_5)(CO)_{15}$ (5a)

Crystals of **5a** were grown by slow evaporation of a dichloromethane:hexane (60:40) mixture and a suitable single crystal was mounted on a glass fibre epoxy resin.

Crystal data

$C_{25}H_{15}Os_5Rh$, $M = 1609.3$, monoclinic, space group $P2_1/n$ (alt. setting $P2_1/c$, No. 14), $a = 9.014(3)$, $b = 30.547(10)$, $c = 11.511(4)$ Å, $\beta = 107.31(3)°$, $V = 3026(2)$ Å^3 (by least-squares refinement of diffractometer angles from 30 automatically centred reflections in the range $15 < 2\theta < 25°$, $\lambda = 0.71073$ Å), $Z = 4$, $D_c = 3.53$ g cm^{-3}, D_m = not measured, $F(000) = 2840$. Purple block. Crystal dimensions: $0.18 \times 0.26 \times 0.50$ mm, μ(Mo Kα) = 215.43 cm^{-1}, $\mu R = 3.38$.

Data collection and processing

Nicolet R3mV diffractometer, 96-step ω–2θ scan mode, with scan range from 0.9° below Kα_1 to 0.9° above Kα_2, with ω scan speeds in the range 3.0–29.3°/min, graphite-monochromated Mo Kα radiation; 4438 reflections measured ($5.0 < 2\theta < 45.0°$, $+h$, $+k$, $\pm l$), 3921 unique (merging $R = 0.011$ after a semi-empirical absorption correction based on an ellipsoid model and 357 scan data (maximum minimum transmission factors 0.018, 0.003), giving 3365 with $F > 4\sigma(F)$. Three check reflections showed no significant variations in intensity during data collection.

TABLE 1. Atomic coordinates ($\times 10^4$) for **4a**

	x	y	z
Os(1)	565(5)	8575(2)	3869(3)
Os(2)	−2051(5)	7935(2)	3559(3)
Os(3)	93(5)	7120(2)	4273(3)
Os(4)	256(4)	7504(2)	2560(3)
Os(5)	−1752(5)	6498(2)	2969(3)
Ru(1)	1164(10)	6092(5)	3355(7)
C(11)	2460(69)	8218(125)	3959(254)
O(11)	3767(17)	8350(134)	4087(182)
C(12)	437(107)	9040(51)	4960(33)
O(12)	416(77)	9342(38)	5619(25)
C(13)	−42(170)	9391(59)	3191(87)
O(13)	−385(59)	9859(23)	2720(34)
C(21)	−3519(56)	7433(27)	4118(53)
O(21)	−4658(45)	7277(32)	4339(44)
C(22)	−2665(164)	8805(25)	4131(69)
O(22)	−2723(111)	9198(38)	4764(57)
C(23)	−3014(122)	8383(82)	2592(53)
O(23)	−3565(69)	8626(41)	1969(30)
C(31)	1742(52)	7447(50)	4902(59)
O(31)	2822(46)	7597(45)	5239(49)
C(32)	−1120(105)	7129(59)	5213(53)
O(32)	−1937(283)	7036(125)	5742(141)
C(33)	444(139)	6201(25)	4815(49)
O(33)	659(87)	5692(25)	5250(49)
C(41)	−97(114)	8310(35)	1806(53)
O(41)	−441(70)	8747(28)	1292(37)
C(42)	2234(16)	7658(48)	2662(54)
O(42)	3445(15)	7726(42)	2639(54)
C(43)	447(220)	6897(46)	1572(37)
O(43)	289(103)	6560(45)	929(35)
C(51)	−1542(101)	5644(30)	2289(48)
O(51)	−1483(91)	5161(31)	1804(49)
C(52)	−2871(99)	6014(86)	3776(81)
O(52)	−3422(74)	5712(40)	4327(43)
C(53)	−3284(57)	6789(94)	2206(60)
O(53)	−4303(57)	6838(49)	1754(47)
C(2)	3576(62)	6027(33)	3230(42)
C(3)	3216	5548	3883
C(4)	2205	5009	3711
C(5)	1555	4949	2885
C(6)	1915	5429	2231
C(1)	2926	5968	2404

Structure solution and refinement

Centrosymmetric direct methods (Os and Rh atoms) followed by Fourier difference techniques for the remaining non-hydrogen atoms. Full-matrix least-squares refinement with Os, Rh, O and cyclopentadienyl C atoms anisotropic. Methyl H atoms were placed in calculated positions (C–H 0.96 Å) and allowed to ride on the relevant carbon; they were refined with a common thermal parameter of 0.13(4) Å^2. The weighting scheme $w = [\sigma^2(F) + 0.003F^2]^{-1}$, with $\sigma(F)$ from counting statistics, gave satisfactory agreement analyses. Final R and R_w values were 0.055 and 0.067, and the goodness of fit parameter $S = 1.57$. Highest peak in the final difference map 1.99 e Å^{-3} close to the metal atom

TABLE 2. Atomic coordinates ($\times 10^4$) for **5a**

	x	y	z
Os(1)	1813(1)	1436(1)	7673(1)
Os(2)	4766(1)	1793(1)	8362(1)
Os(3)	3723(1)	1374(1)	6197(1)
Os(4)	4338(1)	894(1)	8331(1)
Os(5)	1833(1)	677(1)	6323(1)
Rh(1)	3466(2)	1385(1)	10060(2)
C(1)	2417(33)	1018(7)	11221(20)
C(2)	1870(31)	1456(7)	11143(24)
C(3)	3259(29)	1712(9)	11649(22)
C(4)	4513(34)	1472(9)	12015(22)
C(5)	4088(26)	1024(9)	11721(21)
C(6)	1406(37)	652(8)	10973(22)
C(7)	276(36)	1607(11)	10815(35)
C(8)	3153(34)	2220(9)	11877(30)
C(9)	6090(33)	1590(9)	12790(26)
C(10)	5022(36)	622(9)	12119(27)
C(11)	246(30)	1093(9)	8088(23)
O(11)	−688(20)	932(6)	8300(18)
C(12)	1579(33)	1936(10)	8492(27)
O(12)	1262(24)	2274(6)	8904(18)
C(13)	455(38)	1695(11)	6195(31)
O(13)	−344(28)	1832(7)	5356(19)
C(21)	4251(37)	2366(11)	7963(30)
O(21)	4192(29)	2732(8)	7721(25)
C(22)	5490(32)	2032(9)	9965(27)
O(22)	6179(33)	2168(8)	10835(21)
C(23)	6758(36)	1823(10)	8193(29)
O(23)	7898(22)	1836(9)	7936(26)
C(31)	2566(47)	1231(14)	4621(40)
O(31)	1950(43)	1139(13)	3608(24)
C(32)	3611(36)	1982(12)	5537(30)
O(32)	3535(45)	2270(8)	5161(29)
C(33)	5612(39)	1230(11)	5912(31)
O(33)	6762(29)	1151(11)	5739(27)
C(41)	3636(31)	426(9)	8947(25)
O(41)	3209(25)	89(7)	9395(21)
C(42)	6077(31)	1021(9)	9710(25)
O(42)	7202(22)	1008(6)	10511(19)
C(43)	5604(43)	538(12)	7667(34)
O(43)	6415(25)	333(6)	7324(21)
C(51)	832(32)	232(10)	6983(26)
O(51)	144(31)	28(10)	7397(21)
C(52)	40(37)	780(10)	5038(31)
O(52)	−1098(27)	795(7)	4206(22)
C(53)	2761(40)	264(12)	5545(33)
O(53)	3184(32)	−24(9)	5082(31)

positions. Final fractional atomic coordinates are presented in Table 2. Computations were carried out on a Micro Vax II computer using the SHELXTL PLUS package [9].

Results and discussion

The low temperature, dropwise addition of the cluster dianion $[Os_5(CO)_{15}]^{2-}$ (as its $[(Ph_3P)_2N]^+$ salt) (**1**), in dichloromethane, to a solution containing one equivalent of the dication $[Ru(C_6H_6)(MeCN)_3]^{2+}$ (as its PF_6^- or BF_4^- salt) led to the isolation of two red–brown isomers of the same cluster $RuOs_5(CO)_{15}(\eta^6\text{-}C_6H_6)$ (**4**). In a similar manner, the $[Rh(C_5Me_5)(MeCN)_3]^{2+}$ dication (as its PF_6^- salt) reacted with **1** to yield three isomers of the heterometal cluster $RhOs_5(CO)_{15}(\eta^5\text{-}C_5Me_5)$ (**5**). The yields of the individual isomers **5a**, **5b** and **5c** were dependent on the reaction times, with an increase in the proportions of **5b** and **5c** formed if the reaction was continued for more than 1 h. On dissolving pure samples of either **5a**, **5b** or **5c** in dichloromethane conversion to a mixture of all three compounds occurred, confirming that they were indeed isomers of the same cluster.

Compounds **4** and **5** were initially characterised from spectroscopic data which is presented in Table 3. Electron impact mass spectroscopy results confirm that hexanuclear clusters have been formed. The IR spectral carbonyl stretching frequencies of the individual isomers of **4** and **5** could not be obtained for the pure forms but it would appear that they are very similar indicating that they all probably possess the same central metal core geometry.

NMR data (^1H and ^{13}C) for **4** indicates that two isomers are present in solution, exhibiting singlets at δ 5.92 and δ 5.84 (C_6H_6) in the ^1H NMR and δ 86.3 and δ 85.6 in the ^{13}C NMR spectrum in an isomeric ratio of 1:1. The position of the resonances is diagnostic for η^6-coordination of the benzene ligand to one metal [4], with the singlet structure indicating equilibration of all sites on the ring occurs by rapid rotation. Variable temperature NMR studies do not show evidence of any change in the isomeric ratio of 1:1 over the temperature range 90 to −90 °C. This suggests the presence of two non-interconverting isomeric forms; any existing interconversion process must necessarily be of very low energy.

The isomers of complex **5** all exhibit a characteristic singlet at δ 1.27 for the $\eta^5\text{-}C_5(CH_3)_5$ protons in the ^1H NMR spectrum at 30 °C, where again rapid rotation of the ligand is evidenced by the singlet structure of the resonance. This indicates that interconversion between the three isomeric forms is occurring at room temperature. Insufficient material was obtained for a ^{13}C NMR spectroscopic study to be undertaken.

The formulation of the complexes **4** and **5** suggests that they are isoelectronic with the hexanuclear osmium cluster, $Os_6(CO)_{18}$ [6], in which there are three different classes of metal atom displaying different metal connectivities of 3, 4 and 5, respectively. These different classes of metal atoms are formally considered as being 17, 18 and 19 electron centres, respectively. In the mixed-metal clusters **4** and **5**, occupancy of these different metal sites in the bicapped tetrahedron is suggested as a possible rationalisation of the observed isomerism.

TABLE 3. Spectroscopic data for the new complexes **4**, **5**, **6** and **7**

Compound	IR[a] ν_{CO} (cm^{-1})	MS (m/e)[b] exp., calc.	^1H NMR[c] δ (ppm)	^{13}C NMR[c] δ (ppm)
4a, b	2087w, 2054m, 2026s 1999w, 1988w, 1975w	1560, 1560	5.92s (6H) 5.84s (6H)	86.3 85.6
5a	2079m, 2047m, 2018vs 1938m, br	1616, 1618	1.26s (15H)	
5b	as for **5a**			
5a	as for **5a**			
6	[d]2026m, 1977s, 1962s 1897m, br			
7	2085w, 2055m, 2017vs 1997m, 1975w, 1955s 1944m	2160, 2160	5.57s (6H) 2.13m (12H) 1.33m (18H) −71.2s (^{31}P)[e] −57.1s (^{31}P)[e]	

s = strong; m = medium; w = weak; br = broad; sh = shoulder. [a]Spectrum run in hexane. [b]$M+(m/e)$ based on ^{192}Os. [c]Spectrum run in $CDCl_3$. [d]Spectrum run in THF. [e]Referenced to δ $P(OMe)_3$.

Reduction of a mixture of **4a** and **4b** with K/Ph_2CO or Na/Hg in tetrahydrofuran produces the dianionic cluster $[RuOs_5(CO)_{14}(\eta^6\text{-}C_6H_6)]^{2-}$ (**6**) in high yield. This is a highly unstable, oxygen sensitive anion which has been characterised on the basis of its spectroscopic data (the ν(CO) stretching frequencies in the IR spectrum move to lower wavenumbers (Table 3), as expected for an anionic cluster), and from its reaction with $[AuPEt_3]Cl/TlBF_4$ to form the compound $RuOs_5(CO)_{14}(\eta^6\text{-}C_6H_6)(AuPEt_3)_2$ (**7**). This cluster has been fully characterised by IR, mass spectroscopy, ^1H and ^{13}P NMR analyses. In the ^1H NMR spectrum, the singlet at δ 5.57, attributable to the six equivalent ring protons, is ~0.3 ppm upfield relative to the parent compound, however, is still within the region associated with η^6-coordination to one metal vertex. The upfield shift reflects a small increase in electron density, presumably from the strong σ- donor PR_3 ligands, transmitted through the $RuOs_5Au_2$ cluster framework. The ^{31}P NMR spectrum exhibits two singlets at $\delta -57.1$ and $\delta -71.2$, indicating the inequivalence of the gold ligand environments. By comparison to **6** the homometallic cluster, $[Os_6(CO)_{18}]^{2-}$, adds two $AuPR_3$ units to form a *trans*-bicapped octahedron [2]. Assuming an octahedral geometry is adopted by $[RuOs_5(CO)_{14}(C_6H_6)]^{2-}$ (**6**), a similar 1,4-*trans*-capping arrangement would be consistent with the ^{31}P NMR data but may be disfavoured by steric crowding by the arene ring. A 1,2*cis*-capped structure may be preferred while still accommodating the non-equivalence of the ^{31}P NMR resonances.

In an attempt to form the dihydride $RuOs_5(CO)_{14}(H_2)$, the dianion $[RuOs_5(CO)_{14}(\eta^6\text{-}C_6H_6)]^{2-}$ (**6**) was treated with $HBF_4 \cdot Et_2O$ but decomposition occurred and the parent cluster **4** was obtained in small amounts.

By comparison to complex **4**, $Os_6(CO)_{18}$ readily forms a stable dianion by reduction with a range of nucleophiles and reductants [2]. The homometallic anion $[Os_6(CO)_{18}]^{2-}$, adopts an octahedral arrangement, appropriate to an 86 electron cluster by PSEP theory [10]. A similar structural change may occur upon reduction of the mixed-metal system **4**. In this case, however, the stability of the anion has been dramatically decreased by introduction of the 'Ru(C_6H_6)' fragment. Addition of electrons to the neutral cluster **4**, a process commonly associated with metal–metal bond cleavage, may induce a transformation to the open type of structure recently observed for $Ru_6(\mu^4\text{-}\eta^2\text{-}CO)_2(CO)_{13}(\eta^6\text{-}C_6H_3Me_3)$ [11]. The IR data for the reversible reduction of **4**, however, does not provide evidence of the formation of a compound similar to $Ru_6(\mu^4\text{-}\eta^2\text{-}CO)_2(CO)_{13}(\eta^6\text{-}C_6H_3Me_3)$, rather it exhibits a clean conversion to a compound which is isostructural to the parent cluster. The simplicity of the ν(CO) bands in the IR spectrum and the inferred symmetry of the structure suggests that a bicapped-tetrahedron to [octahedron]$^{2-}$ interconversion is the most likely rationale.

Crystallographic discussion

Single crystals, suitable for X-ray analysis were obtained for the clusters $RuOs_5(CO)_{15}(\eta^6\text{-}C_6H_6)$ (**4a**) and $RhOs_5(CO)_{15}(\eta^5\text{-}C_5Me_5)$ (**5a**), and it was assumed that crystallisation of the thermodynamically preferred structure occurred in both systems. The results of the crystallographic analyses on the clusters **4a** and **5a** showed that in both molecules the metal framework is best described as a bicapped tetrahedron in which the heterometallic fragment adopts a capping position in the polyhedron. The bicapped tetrahedral geometry has previously been observed in the parent osmium

binary carbonyl, $Os_6(CO)_{18}$ [3], and a number of its derivatives [12].

The molecular structure of $RuOs_5(CO)_{15}(\eta^6\text{-}C_6H_6)$ (**4a**) is shown in Fig. 1, while that of $RhOs_5(CO)_{15}(\eta^5\text{-}C_5Me_5)$ (**5a**) is shown in Fig. 2. Selected bond parameters for the two molecules are presented in Tables 4 and 5, respectively. An analysis of the molecular packing for both complexes shows that there are no abnormally short intermolecular contacts between molecules and that the discrete units are separated by normal van der Waals' distances.

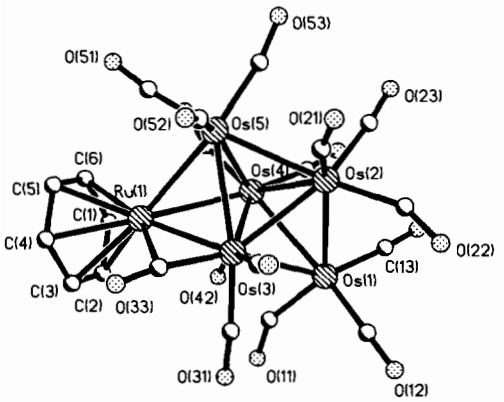

Fig. 1. The molecular structure of $RuOs_5(CO)_{15}(\eta^6\text{-}C_6H_6)$ (**4a**) showing the atom numbering scheme.

In the metal frameworks of the bicapped tetrahedral clusters of osmium [3, 12], it is observed that there is a metal–metal edge lengthening between metals with formally different electron counts. In the clusters **4a** and **5a**, however, the major bond length variations relate to the heterometallic metal–metal distances compared to the homometallic metal–metal edge lengths (Tables 4 and 5). For **5a**, the shortest edge length is between the two 18 electron centres (Os(2)–Os(3)), as seen in $Os_6(CO)_{18}$, while a bond lengthening of 0.09 Å is observed for the 18 electron–17 electron site interaction (Os(2)–Rh(1)) due to introduction of the heterometallic fragment, compared to the value for the Os(3)–Os(5) edge. One of the 19 electron centre–17 electron centre interactions (Os(1)–Rh(1)) is shortened by 0.07 Å in this molecule compared to other interactions involving Rh(1). This shortening can formally be associated with a dative bond, however, atypically, no incipient carbonyl ligand is present to support this bond. In the complex **4a**, the 19 electron–17 electron metal distances show even greater variation, however all bond lengths in this molecule show a larger variation which should be analysed with the caveat that the crystallographic data set for this molecule is less precise. With this in mind, there is still a significant difference between the edge lengths of Ru(1)–Os(3) (2.599(10) Å) and Ru(1)–Os(4) (2.975(10) Å), especially in relation to the equivalent

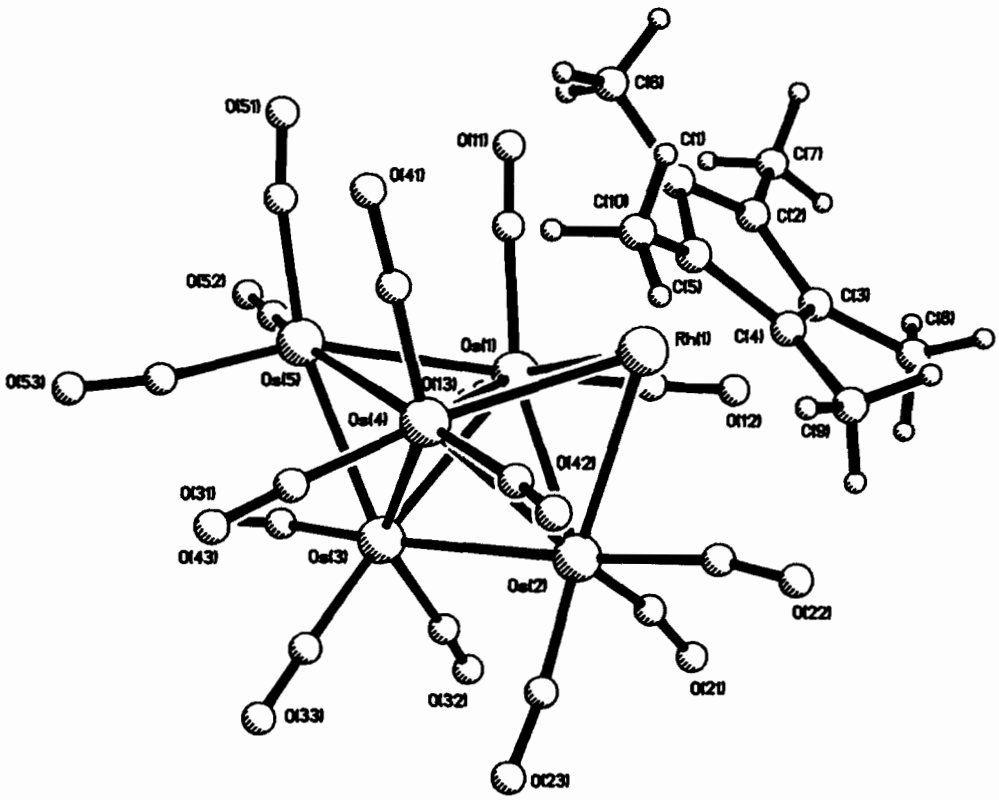

Fig. 2. The molecular structure of $RhOs_5(CO)_{15}(\eta^5\text{-}C_5Me_5)$ (**5a**) showing the atom numbering scheme.

TABLE 4. Selected bond lengths (Å) and angles (°) for $RuOs_5(CO)_{15}(\eta^6\text{-}C_6H_6)$ (**4a**)

Os(1)–Os(2)	2.772(6)	Os(1)–Os(3)	2.780(6)
Os(1)–Os(4)	2.824(6)	Os(2)–Os(3)	2.716(6)
Os(2)–Os(4)	2.859(6)	Os(2)–Os(5)	2.807(6)
Os(3)–Os(4)	2.753(6)	Os(3)–Os(5)	2.845(7)
Os(3)–Ru(1)	2.599(10)	Os(4)–Os(5)	2.753(6)
Os(4)–Ru(1)	2.975(10)	Os(5)–Ru(1)	2.906(10)
Ru(1)–C(1)	2.30(6)	Ru(1)–C(2)	2.32(6)
Ru(1)–C(3)	2.31(7)	Ru(1)–C(4)	2.27(7)
Ru(1)–C(5)	2.25(6)	Ru(1)–C(6)	2.27(7)
Os(3)–Os(1)–Os(2)	58.6(2)	Os(4)–Os(1)–Os(2)	61.4(2)
Os(4)–Os(1)–Os(3)	58.8(2)	Os(3)–Os(2)–Os(1)	60.9(2)
Os(4)–Os(2)–Os(1)	60.2(2)	Os(4)–Os(2)–Os(3)	59.1(2)
Os(5)–Os(2)–Os(1)	110.4(2)	Os(5)–Os(2)–Os(3)	62.0(2)
Os(5)–Os(2)–Os(4)	58.1(2)	Os(2)–Os(3)–Os(1)	60.6(2)
Os(4)–Os(3)–Os(1)	61.4(2)	Os(4)–Os(3)–Os(2)	63.0(2)
Os(5)–Os(3)–Os(1)	109.1(2)	Os(5)–Os(3)–Os(2)	60.6(2)
Os(5)–Os(3)–Os(4)	58.9(2)	Ru(1)–Os(3)–Os(1)	120.0(3)
Ru(1)–Os(3)–Os(2)	118.9(3)	Ru(1)–Os(3)–Os(4)	67.5(3)
Ru(1)–Os(3)–Os(5)	64.3(3)	Os(2)–Os(4)–Os(1)	58.4(2)
Os(3)–Os(4)–Os(1)	59.8(2)	Os(5)–Os(4)–Os(1)	110.5(2)
Os(5)–Os(4)–Os(2)	60.0(1)	Os(5)–Os(4)–Os(3)	62.2(2)
Ru(1)–Os(4)–Os(1)	106.9(3)	Ru(1)–Os(4)–Os(2)	103.4(2)
Ru(1)–Os(4)–Os(3)	53.8(2)	Ru(1)–Os(4)–Os(5)	60.8(2)
Os(3)–Os(5)–Os(2)	57.4(2)	Os(4)–Os(5)–Os(2)	61.9(2)
Os(4)–Os(5)–Os(3)	58.9(2)	Ru(1)–Os(5)–Os(2)	106.5(2)
Ru(1)–Os(5)–Os(3)	53.7(2)	Ru(1)–Os(5)–Os(4)	63.4(2)
Os(4)–Ru(1)–Os(3)	58.7(2)	Os(5)–Ru(1)–Os(3)	61.9(2)
Os(5)–Ru(1)–Os(4)	55.8(2)		

TABLE 5. Selected bond lengths (Å) and angles (°) for $RhOs_5(CO)_{15}(\eta^5\text{-}C_5Me_5)$ (**5a**)

Os(!)–Os(2)	2.765(2)	Os(1)–Os(3)	2.762(2)
Os(1)–Os(4)	2.733(2)	Os(1)–Os(5)	2.794(2)
Os(1)–Rh(1)	2.712(2)	Os(2)–Os(3)	2.709(2)
Os(2)–Os(4)	2.771(2)	Os(2)–Rh(1)	2.848(3)
Os(3)–Os(4)	2.771(2)	Os(3)–Os(5)	2.758(2)
Os(4)–Os(5)	2.788(2)	Os(4)–Rh(1)	2.784(3)
Rh(1)–C(1)	2.17(3)	Rh(1)–C(2)	2.18(3)
Rh(1)–C(3)	2.14(3)	Rh(1)–C(4)	2.18(2)
Rh(1)–C(5)	2.13(2)	C(1)–C(2)	1.42(3)
C(1)–C(5)	1.44(4)	C(2)–C(3)	1.44(3)
C(3)–C(4)	1.31(4)	C(4)–C(5)	1.43(4)
Os(2)–Os(1)–Os(3)	58.7(1)	Os(2)–Os(1)–Os(4)	60.5(1)
Os(3)–Os(1)–Os(4)	60.6(1)	Os(2)–Os(1)–Os(5)	108.8(1)
Os(3)–Os(1)–Os(5)	59.5(1)	Os(4)–Os(1)–Os(5)	60.6(1)
Os(2)–Os(1)–Rh(1)	62.6(1)	Os(3)–Os(1)–Rh(1)	111.3(1)
Os(4)–Os(1)–Rh(1)	61.5(1)	Os(5)–Os(1)–Rh(1)	115.0(1)
Os(1)–Os(2)–Os(3)	60.6(1)	Os(1)–Os(2)–Os(4)	59.2(1)
Os(3)–Os(2)–Os(4)	60.7(1)	Os(1)–Os(2)–Rh(1)	57.8(1)
Os(3)–Os(2)–Rh(1)	108.9(1)	Os(4)–Os(2)–Rh(1)	59.4(1)
Os(1)–Os(3)–Os(2)	60.7(1)	Os(1)–Os(3)–Os(4)	59.2(1)
Os(2)–Os(3)–Os(4)	60.7(1)	Os(1)–Os(3)–Os(5)	60.8(1)
Os(2)–Os(3)–Os(5)	111.5(1)	Os(4)–Os(3)–Os(5)	60.6(1)
Os(1)–Os(4)–Os(2)	60.3(1)	Os(1)–Os(4)–Os(3)	60.3(1)
Os(2)–Os(4)–Os(3)	58.5(1)	Os(1)–Os(4)–Os(5)	60.8(1)
Os(2)–Os(4)–Os(5)	108.8(1)	Os(3)–Os(4)–Os(5)	59.5(1)
Os(1)–Os(4)–Rh(1)	58.9(1)	Os(2)–Os(4)–Rh(1)	61.7(1)
Os(3)–Os(4)–Rh(1)	109.0(1)	Os(5)–Os(4)–Rh(1)	112.9(1)
Os(1)–Os(5)–Os(3)	59.7(1)	Os(1)–Os(5)–Os(4)	58.6(1)
Os(3)–Os(5)–Os(4)	59.9(1)	Os(1)–Rh(1)–Os(2)	59.6(1)
Os(1)–Rh(1)–Os(4)	59.6(1)	Os(2)–Rh(1)–Os(4)	58.9(1)

homometallic bond lengths of *c.* 2.80 Å. The shorter bond is supported by an incipient bridging carbonyl ligand, exhibiting a –CO...M contact distance of 2.40(9) Å and a deviation from linearity of the M–C–O angle (171(6)°). This perturbation of the electron distribution is further expressed in the edge lengthening between the 18 electron centres Os(2) and Os(5) (2.807(6) Å), relative to that between the 19 electron centres Os(3) and Os(4) (2.753(6) Å). Variation of the heterometallic cap–basal interactions relative to the homometallic relation is again observed, and is of the order of 0.13 Å. The dihedral angle of the plane of the cyclic hydrocarbon ligands relative to the capped face of the central tetrahedron is similar; for benzene substituted cluster **4a** an angle of 10.9° is observed, while for **5a** the C_5Me_5 ligand is tilted by 9.4° relative to the same face.

Significantly, the extremely short edge length between the 19 electron centre Os(3) and the Ru(1) atom (2.599(10) Å), in **4a** may be an indirect reflection of the dominance of the backbonding requirements of the benzene moiety, causing polarisation of electron density from the electron rich metal centre and perturbation of the electron distribution as reflected in the edge length variation already mentioned. The incipient bridging carbonyl ligand supporting this bond can be interpreted as further satisfying the π-acidity of the $Ru(C_6H_6)$ centre, by delocalisation of electron density between the inequivalent sites.

Using PSEP theory [10], as skeletal electron pair count of 6 for the hexanuclear system predicts a capped trigonal bipyramid, or bicapped tetrahedron, as is observed. This polytope for $S=6$ is considered an electron deficient cluster, as, according to the borane analogy, a *closo* cluster of n vertices requires $n+1$ skeletal electron pairs. The formation of the heterometallic clusters can therefore be rationalised, both mechanistically and theoretically by the capping principle [13].

Supplementary material

Tables of thermal parameters, hydrogen atom coordinates, full lists of bond parameters, and tables of structure factors for the crystal structures (of **4a** and **5a**) are available from the authors.

Acknowledgement

We gratefully acknowledge the financial support of Christ's College, Cambridge (P.A.J.).

References

1 P. Chini and B. T. Heaton, *Top. Curr. Chem., 71* (1977) 1; W. L. Gladfelter and G. L. Geoffroy, *Adv. Organomet. Chem., 18* (1980) 207; A. R. Manning, *J. Chem. Soc. A,* (1970) 2321; S. P. Gubin, N. M. Mikova, M. Ts. Tsybenov and V. E. Lopatin, *Koord, Khim., 10* (1984) 625; M. I. Bruce, *J. Organomet. Chem., 257* (1983) 417; J. S. Plotkin, D. G. Alway, C. R. Weisenberger and S. G. Shore, *J. Am. Chem. Soc., 102* (1980) 6157; J. R. Shapley, G. A. Pearson, M. Tachikawa, G. Schmidt, M. R. Churchill and F. J. Hollander, *J. Am. Chem. Soc., 99* (1977) 8064.

2 J. N. Nicholls and M. D. Vargas, *Adv. Inorg. Chem. Radiochem., 30* (1986) 123; I. D. Salter, *Adv. Organomet. Chem., 29* (1989) 249.

3 B. F. G. Johnson, R. D. Johnson and J. Lewis, *J. Chem. Soc. A,* (1968) 2865; R. Mason, K. M. Thomas and D. M. P. Mingos, *J. Am. Chem. Soc., 95* (1973) 3802.

4 B. F. G. Johnson, J. Lewis, M. P. Gomez-Sal, P. R. Raithby and A. H. Wright, *J. Chem. Soc., Chem. Commun.,* (1985) 1682; P. Bailey, B. F. G. Johnson and J. Lewis, *J. Chem. Soc., Chem. Commun.,* (1989) 2865.

5 M. A. Bennett and A. K. Smith, *J. Chem. Soc., Dalton Trans.,* (1974) 233.

6 C. White, S. J. Thompson and P. M. Maitlis, *J. Chem. Soc.,* (1977) 1654.

7 C. R. Eady, J. J. Guy, B. F. G. Johnson, J. Lewis, M. C. Malatesta and G. M. Sheldrick, *J. Chem. Soc., Chem. Commun.,* (1976) 807.

8 C. A. McAuliffe, R. V. Parish and P. D. Randall, *J. Chem. Soc., Dalton Trans.,* (1979) 1730.

9 G. M. Sheldrick, *SHELXTL PLUS,* an integrated system for solving, refining, and displaying crystal structures from diffraction data, University of Göttingen, FRG, 1986.

10 K. Wade, *J. Chem. Soc., Chem. Commun.,* (1971) 792; (b) *Adv. Inorg. Chem. Radiochem., 18* (1976) 1; K. Wade, in B. F. G. Johnson (ed.), *Transition Metal Clusters,* Wiley, New York, 1980, p. 193.

11 C. E. Anson, P. J. Bailey, G. Conole, B. F. G. Johnson, J. Lewis, M. McPartlin and H. R. Powell, *J. Chem. Soc., Chem. Commun.,* (1989) 442.

12 A. G. Orpen and G. M. Sheldrick, *Acta Crystallogr., Sect. B, 34* (1978) 1989; C. Courture, D. H. Farrar, M. P. Gomez-Sal, B. F. G. Johnson, R. A. Kamarudin, J. Lewis and P. R. Raithby, *Acta Crystallogr., Sect. C, 42* (1986) 163; B. F. G. Johnson, R. A. Kamarudin, F. J. Lahoz, J. Lewis and P. R. Raithby, *J. Chem. Soc., Dalton Trans.,* (1988) 1205.

13 C. R. Eady, B. F. G. Johnson and J. Lewis, *J. Chem. Soc., Dalton Trans.,* (1975) 2606; M. McPartlin, *Polyhedron, 3* (1984) 1279.